DYNAMIC MODELING OF A HIGH-PRESSURE PUMP CONSIDERING NON-DELIVERY ANGLE FOR MODEL-BASED DIAGNOSIS OF COMMON RAIL SYSTEMS

MÔ HÌNH HOÁ ĐỘNG LỰC HỌC BƠM CAO ÁP XÉT ĐẾN GÓC KHÔNG PHÂN PHỐI PHỤC VỤ CHẨN ĐOÁN LỖI THEO MÔ HÌNH CHO HỆ THỐNG PHUN NHIÊN LIỆU COMMON RAIL

Nguyen Hoang Vu*, Nguyen Tat Trong, Tran Phuc Hoang

Le Quy Don Technical University, Vietnam

*Corresponding author: vunguyenhoang@lqdtu.edu.vn

(Received: April 01, 2026; Revised: April 30, 2026; Accepted: May 22, 2026)

DOI: 10.31130/ud-jst.2026.24(5A).201E

Abstract - In diesel Common Rail systems, the actual delivery flow of the high-pressure pump (HPP) is typically lower than its theoretical value due to incomplete fuel filling, which is characterized by the non-delivery angle (X_{nd}). This paper evaluates and simulates the HPP characteristics for a Hyundai D4CB 2.5 TCI-A engine, incorporating control parameters from the ECU and accounting for the influence of X_{nd}. Implemented in Matlab/Simulink, the simulation results indicate that when the engine speed exceeds approximately 2000 rpm, X_{nd} increases significantly, leading to a decline in actual pump flow. This reduction in flow directly disrupts the dynamic equilibrium of the system, causing deviations in the rail pressure signal (p_{cr}) - the critical parameter for diagnosing the high-pressure circuit. Integrating the X_{nd} parameter into the reference model ensures the accurate prediction of rail pressure dynamics, thereby serving as a basis for developing Model-Based Diagnosis algorithms.

Key words - CP1-H high-pressure pump; Non-delivery angle; Volumetric efficiency; Rail pressure; Model-Based Diagnosis

Tóm tắt - Trong hệ thống phun nhiên liệu diesel kiểu Common Rail, lưu lượng cung cấp thực tế của bơm cao áp (BCA) thường thấp hơn giá trị lý thuyết do hiện tượng nạp nhiên liệu không hoàn toàn, được đặc trưng bởi góc không phân phối (X_{nd}). Bài báo này tiến hành mô phỏng và đánh giá đặc tính cung cấp của BCA trên động cơ Hyundai D4CB 2.5 TCI-A, có xét đến các thông số điều khiển từ ECU và sự ảnh hưởng của X_{nd}. Kết quả mô phỏng trên Matlab/Simulink cho thấy khi tốc độ động cơ vượt ngưỡng khoảng 2000 vg/ph, góc X_{nd} tăng lên đáng kể, dẫn đến sự sụt giảm lưu lượng của BCA. Sự sụt giảm này phá vỡ trạng thái cân bằng động của hệ thống, gây ra các sai lệch trực tiếp đối với tín hiệu áp suất rail (p_{cr}) - thông số cốt lõi được sử dụng để chẩn đoán mạch cao áp. Việc tích hợp tham số X_{nd} vào mô hình giúp dự đoán chính xác động học của tín hiệu p_{cr}, qua đó làm cơ sở để phát triển các thuật toán chẩn đoán lỗi theo mô hình.

Từ khóa - Bơm cao áp CP1-H; Góc không phân phối; Hiệu suất thể tích; Áp suất ống rail; Chẩn đoán theo mô hình

1. Introduction

In modern diesel engines, the Common Rail (CR) fuel injection system is widely utilized due to its capability to generate high injection pressures independently of engine speed, thereby significantly improving thermal efficiency and reducing exhaust emissions. The high-pressure pump (HPP) is a core component of this system, responsible for generating and maintaining the required fuel pressure in the accumulator (rail) to ensure precise fuel atomization and distribution [1-3].

As the complexity of CR systems increases to meet increasingly stringent emission standards, ensuring their reliability and operational stability becomes a major challenge. Traditional On-Board Diagnostics (OBD), which primarily rely on limit-checking and plausibility checks of sensor signals, are often insufficient for early and detailed fault detection. Consequently, Model-Based Diagnosis (MBD) has emerged as a highly promising approach. By employing mathematical models that describe the physical dynamics of the system, MBD compares predicted output signals from a reference model with actual sensor measurements. The discrepancies between them generate "residuals," which serve as analytical symptoms for fault detection and isolation [4-6].

Within the MBD architecture for the CR high-pressure circuit, the rail pressure (p_{cr}) signal serves as the most critical diagnostic parameter. This signal reflects the dynamic equilibrium among the fuel supplied by the HPP, the fuel discharged via the pressure control valve (PCV), and the fuel consumed by the injectors [3, 7]. Since both HPP delivery and injection events are discontinuous, they induce characteristic pressure oscillations within the rail. Therefore, any degradation in pump volumetric efficiency, system leakage, or actuator deviation will directly manifest as anomalies in the mean value, pressure build-up delay, or alterations in the amplitude and frequency of the p_{cr} signal [8, 9]. Consequently, analyzing pressure fluctuations caused solely by the injectors [10] is insufficient; combining HPP dynamics simulations that consider the non-delivery angle (X_{nd}) is essential for accurate rail pressure prediction and real-time MBD development.

The general structure of an MBD system based on the p_{cr} signal is illustrated in Figure 1. In this architecture, the "reference model" plays a central role by utilizing available ECU control parameters - such as metering valve current (I_{mv}), PCV current (I_{pcv}), engine speed

(n_{eng}), and injected fuel quantity (u_{inj}) - to simulate nominal rail pressure. This approach allows for the isolation of specific component faults, such as HPP plunger damage or individual injector deviations, without requiring additional physical sensors [11, 12].

Despite these diagnostic advantages, developing a reference model that is both highly accurate and computationally optimal remains a significant challenge. Current research often reveals a gap between two extremes: detailed models developed in specialized software like GT-Suite, AMESim, Matlab/Fuzzy Logic Designer [13-17], and simplified analytical models. While the former offer high precision, their heavy computational load makes them unsuitable for real-time MBD applications. Conversely, simplified models often fail to capture critical nonlinear dynamics, particularly the non-delivery angle (X_{nd}). This angle represents the interval during the compression stroke where the internal chamber pressure has not yet exceeded the rail pressure, meaning no fuel is being delivered.

The existence of X_{nd} causes the actual instantaneous flow rate to be significantly lower than the theoretical capacity, compelling the ECU's closed-loop controller to continuously adjust the MV and PCV currents to maintain target pressure [1], [18], [19]. If X_{nd} is not analyzed as an independent variable, the dynamics of the p_{cr} signal and the ECU's control strategy cannot be accurately predicted, inevitably leading to false alarms in the MBD system's residuals.

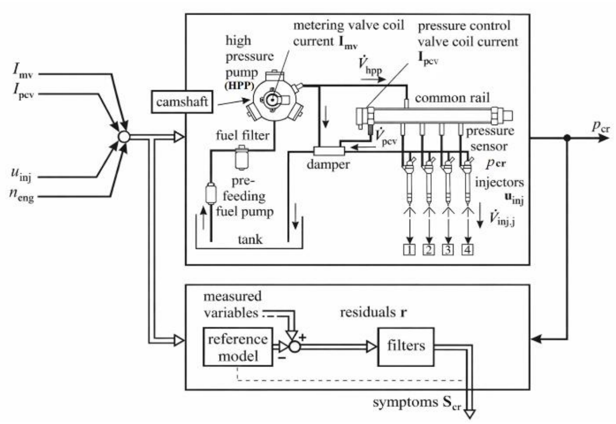

Figure 1. *Structure of the model-based fault diagnosis for CR fuel injection system [8]*

I_{mv}: Metering valve control current; I_{pcv}: Pressure control valve control current; u_{inj}: Injected fuel quantity; n_{eng}: Engine speed; $\dot{V}_{hpp}$ - HPP volume flow; $\dot{V}_{pcv}$: Volume flow through the pressure control valve; $\dot{V}_{inj}$: Injection volume flow of 4 injectors; p_{cr}: Rail pressure; r: Residuals; S_{cr}: Diagnostic symptoms.

To bridge this gap, the present study establishes a streamlined calculation program in the crank angle domain. This approach meets real-time processing requirements while precisely capturing the influence of X_{nd} during incomplete fuel filling at high speeds. Specifically, this paper focuses on evaluating the effect of X_{nd} on the fuel delivery characteristics of a CP1-H HPP equipped on a Hyundai D4CB 2.5 TCI-A diesel engine. By integrating ECU control parameters into a Matlab/Simulink environment, this study establishes a precise relationship between engine speed, effective delivery angle, and actual pump flow rate, providing the essential theoretical foundation for deploying real-time MBD algorithms for CR systems.

2. Research object and experimental setup

The research object of this study is the HPP of the CR fuel injection system on a Hyundai D4CB 2.5 TCI-A engine installed in a Hyundai Starex vehicle. This is a 4-cylinder, 4-stroke, turbocharged diesel engine equipped with a CP1-H HPP, which utilizes a MV for flow control and a PCV for pressure regulation.

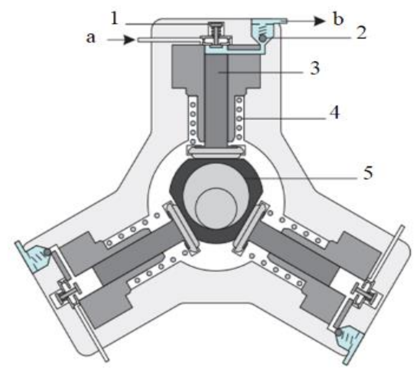

Figure 2. *Schematic diagram of the CP1-H HPP [20]*

1: Inlet valve; 2: Discharge valve; 3: Piston;4: Return spring; 5: Eccentric. a: Connection to the volume in front of the metering valve; b: Connection to the CR.

The CP1-H HPP is a radial piston pump consisting of three pump elements arranged at an offset angle of 120° around the drive shaft [1], [20]. Fuel passes through the MV to control the intake quantity before reaching the inlet valves of the individual pump elements. When the piston moves downwards during the suction stroke, the inlet valve opens, allowing fuel to enter the cylinder chamber. As the piston reaches the bottom dead center (BDC) and begins its upward movement (the compression stroke), the inlet valve closes, causing the fuel to be compressed and the pressure inside the chamber to rise rapidly. As soon as the pressure in the cylinder chamber exceeds the actual pressure in the CR, the discharge valve opens, and the high-pressure fuel is delivered into the rail. The discharge process continues until the piston reaches the top dead center (TDC). Subsequently, the piston begins its downward movement, and the chamber pressure drops rapidly, causing the discharge valve to close in order to prevent fuel from flowing back from the rail. When this pressure drops below the feed pressure supplied by the MV, the inlet valve reopens, and a new cycle begins.

During one revolution of the HPP drive shaft, the three pump elements sequentially perform the suction, compression, and discharge processes, generating overlapping delivery strokes that help stabilize the pump pressure. The maximum delivery rate of the HPP is proportional to the rotational speed of the camshaft; however, the actual fuel quantity delivered into the HPP is strictly determined by the opening cross-section of the MV [20]. The main technical specifications of the HPP are presented in Table 1.

The authors conducted experiments on a Hyundai Starex vehicle using a chassis dynamometer to determine the variation of I_{mv} in the D4CB 2.5 TCI-A engine according to engine speed. The engine speed signal (n_{eng}, rpm) was extracted directly from the ECU via an ELM327 diagnostic tool connected to the OBD-II port. The MV control current I_{mv} was measured using an ACS712 current sensor connected to an Arduino microcontroller board. Data from the ELM327 and Arduino were synchronized in real-time and stored digitally on a computer for subsequent analysis and modeling. To ensure safety, the engine speed was limited to a maximum of 3300 rpm. The measurement results of I_{mv} with respect to engine speed are presented in Table 2.

Table 1. *Main technical specifications of the HPP for the D4CB 2.5 TCI-A engine [2], [20]*

No.	Parameter	Value
1	Low-pressure fuel pump	Electric pump, pressure 5 bar
2	CP1-H high-pressure pump with 3 radial pistons	- Maximum delivery rate: 843 mm³/rev - Maximum rail pressure: 1600 bar
3	Metering valve (MV)	Solenoid valve, normally open

Table 2. *Variation of I_{mv} according to engine speed.*

No.	n_{eng}, rpm	I_{mv}, A
1	800	1.34
2	1500	1.32
3	2000	1.26
4	2500	1.25
5	3000	1.23
6	3300	1.22

3. Dynamic modeling of the high-pressure pump

The MV plays a crucial role in controlling the amount of fuel supplied from the low-pressure supply circuit. The instantaneous volumetric flow rate through the MV (Q_{mv}) is determined based on the fluid dynamics equation [20]:

$$Q_{mv} = C_{mv}.A(x).\sqrt{\frac{2\Delta p}{\rho}} \tag{1}$$

where C_{mv} is the flow coefficient; A(x) is the flow cross-section through the valve (m²); Δp is the pressure difference across the valve (kPa); and ρ is the fuel density (kg/m³).

In equation (1), the coefficient C_{mv} represents the ratio between the actual flow rate and the ideal flow rate. The value $C_{mv} = 1$ is only achieved under perfectly ideal flow conditions (no losses, no friction, no contraction, or swirl) - a state that never occurs given the complex geometric structure of the MV. To simplify the computational model, previous studies have often assumed C_{mv} to be a constant, [21], [22]. Inheriting this approach, this study selects $C_{mv} = 0.7$. Regarding the pressure difference parameter Δp, the pressure upstream of the MV (supplied by the low-pressure electric pump) is consistently maintained within the stable range of 3–5 bar, whereas the pressure downstream of the MV exhibits wave-like oscillations according to the pump's suction cycle, but with a very small amplitude. Based on this operational characteristic, it is reasonable to assume that Δp is virtually constant [11], [12], with its variation primarily due to local losses in the valve area. Therefore, this study selects a fixed value of Δp = 20 kPa. In particular, since the MV is a solenoid valve, its opening cross-section A(x) directly depends on the control current I_{mv}, thereby making I_{mv} the core input parameter for solving the HPP simulation problem [12].

The flow cross-sectional area through the MV is calculated using the following equation:

$$A(x) = \left(1 - \frac{I_{mv}}{I_{mv,max}}\right).A_{mv} \tag{2}$$

During one revolution of the camshaft, each high-pressure pump element delivers a fuel volume equivalent to its effective delivery volume. The variation in fuel volume of a single pump element according to the camshaft angle of the high-pressure pump is determined by the equation [20]:

$$V_{hpp,i}(X_i) = \frac{V_{hpp,max}}{2}(1 - \cos(X_i)) \tag{3}$$

$$X_i = X + (i-1)\cdot\frac{2}{3}\cdot 180° \tag{4}$$

where $V_{hpp,\,max}$ is the maximum volume of one pump element (m³); X_i is the camshaft angle for the i-th pump element (degrees camshaft angle).

The variation in fuel volume in a single pump element of the HPP is determined by the equation:

$$\frac{dV_{hpp,i}}{dX_i} = \frac{V_{hpp,max}}{2} sin\,(X_i) \tag{5}$$

Assuming the fuel volume filled into one pump element is V_{fill}, the volumetric efficiency is determined as:

$$\alpha = \frac{V_{fill}}{V_{hpp,max}} \tag{6}$$

Under the assumption of neglecting fuel compressibility, at the angular position where the pump element starts delivering fuel, $V_{fill} = V_{hpp}$. Combining this with equation (3), the non-delivery angle X_{nd} can be determined by the equation:

$$\alpha.V_{hpp,max} = \frac{V_{hpp,max}}{2}.(1 - \cos\,(X_{nd})) \tag{7}$$

$$X_{nd} = \arccos(1-2\alpha) \tag{8}$$

The angle X_{nd} is measured from the BDC to the point where the piston reaches the geometric start of compression and fuel delivery. Therefore, when setting the camshaft shaft angle within the range of (−180°, 180°), the delivery flow rate of the HPP over time is determined by the equation [20]:

$$\frac{dV_{hpp}}{dX} = \begin{cases} 0, -180 < X_i < X_{nd,i} \\ \sum_{i=1}^{3}\frac{V_{hpp,max}}{2} sin\,(X_i), X_{nd,i} \le X_i \le 180 \end{cases} \tag{9}$$

The relationship between the camshaft angle and the crankshaft angle (φ) over time is expressed as follows:

$$\varphi = \frac{360}{60}.n_{eng}.t \tag{10}$$

$$\chi = \frac{1}{2}\cdot\frac{360}{60}.n_{eng}.t \tag{11}$$

$$\chi_i = \frac{1}{2} \cdot \frac{360}{60} \cdot n_{eng} \cdot t + (i-1) \cdot \frac{2}{3} \cdot 180 \quad (12)$$

$$\frac{d\chi}{dt} = \frac{1}{2} \cdot \frac{360}{60} \cdot n_{eng} \quad (13)$$

The actual volumetric fuel delivery rate of the HPP with respect to time is determined by:

$$\frac{dV_{hpp}}{dt} = \frac{1}{2} \cdot \frac{360}{60} \cdot \begin{cases} 0, -180 < X_i < X_{nd,i} \\ \sum_{i=1}^{3} \frac{V_{hpp,max}}{2} sin\,(X_i), X_{nd,i} \le X_i \le 180 \end{cases} \quad (14)$$

To implement this computational procedure efficiently and systematically, a dedicated algorithm was developed. The overall workflow, which integrates the nonlinear fuel delivery dynamics with the control parameters, is illustrated in the flowchart presented in Figure 3. This structured approach ensures that the calculation of X_{nd} and the resulting pump flow rates are both physically grounded and computationally optimized for real-time diagnostic integration.

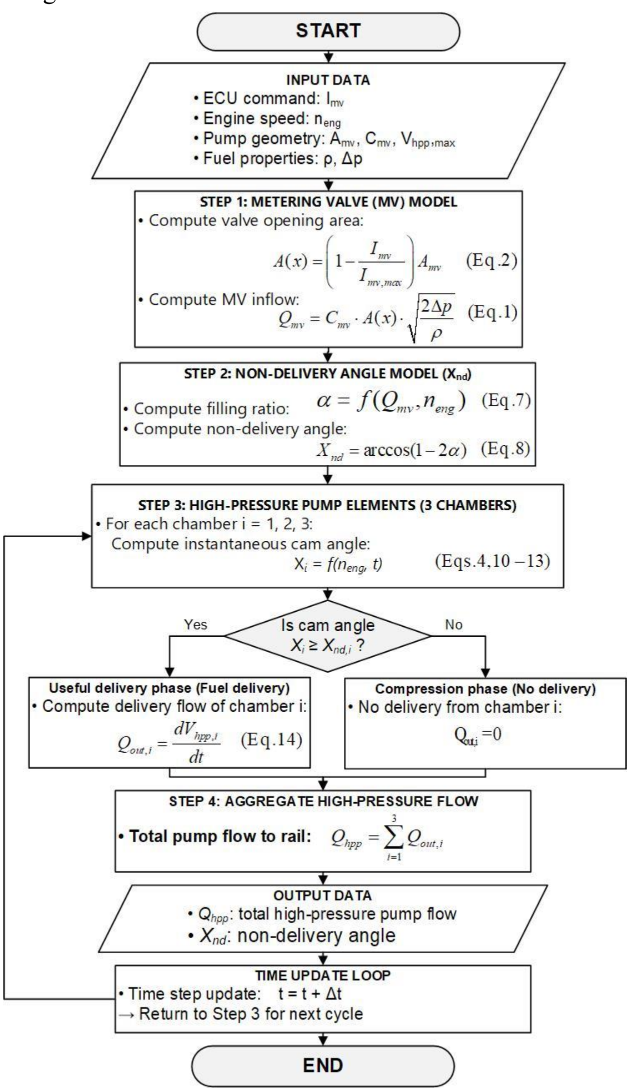

Figure 3. The flowchart for the simulation program

The utilization of X_{nd} allows for evaluating the discrepancy between the actual volumetric flow rate and the theoretical flow rate. Due to the existence of X_{nd}, not the entire compression stroke of the piston constitutes a fuel delivery process, and the actual flow rate is always lower than the ideal calculated value. The fuel flow rate delivered by the HPP primarily depends on: the camshaft speed, the effective flow cross-section of the MV, the low-pressure fuel circuit pressure, and the bulk modulus of the fuel in the pump element cylinder chamber [20]. These factors determine the start of delivery and the actual amount of fuel discharged into the rail, which directly affects the control strategy of the ECU to maintain p_{cr}.

The simulation model of HPP for the D4CB 2.5 TCI-A engine was developed in Matlab/Simulink, with its block diagram illustrated in Figure 4. In this model, the MV block represents the instantaneous volumetric flow rate through the metering valve, determined by equations (1) and (2); the Xnd block represents the non-delivery angle Xnd, calculated using equations (3) to (8); and the pump element blocks are developed based on equations (9) to (14). The main parameters for building the model are presented in Table 3.

Table 3. *Main input parameters of the HPP model [22]*

Symbol	Parameter name	Value
A_{mv}	Maximum flow cross-section of the MV	1.25×10^{-5} (m^2)
C_{mv}	Flow coefficient of the MV	0.7
$V_{hpp,\,max}$	Maximum fuel volume of one pump element	2.694×10^{-7} (m^3)
ρ	Density of diesel fuel at 20°C	830 (kg/m^3)

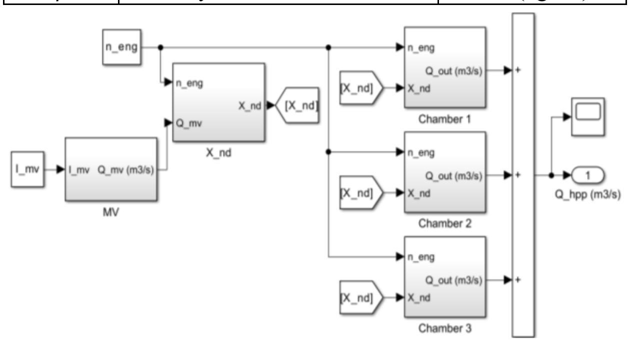

Figure 4. *CP1-H high-pressure pump model developed in Matlab/Simulink*

4. Results and discussion

In HPP simulation studies, many authors have assumed the MV position (corresponding to the control current value I_{mv}) to be constant to simplify the model and isolate the effects of geometric factors or hydraulic conditions of the HPP. When simulating a radial piston HPP with two pump elements, Katharina Prinz [23] utilized a fixed MV position within the range of 0.67 to 0.85; consequently, the fuel delivery capacity of the HPP primarily depended on the MV position and was almost independent of the crankshaft speed. In [2], the authors assumed the control duty cycle of the MV to be within the range of 25% to 33% to analyze rail pressure oscillations and the fuel injection process. Assuming a constant MV opening does not accurately reflect the actual control process of the ECU (Table 2). In practical operation, the ECU adjusts the control currents I_{mv} and I_{pcv} according to the speed and load conditions to optimize the intake flow into the pump element cylinders and maintain the target rail pressure.

The experimental results (Table 2) indicate that I_{mv} varies significantly with speed, decreasing the most in the crankshaft speed range of 2500–3300 rpm. This demonstrates that the assumption of I_{mv} = const is only valid within a narrow range; for a more accurate simulation of the HPP, it is necessary to utilize the I_{mv} control signal from the ECU.

Figure 5 presents the calculated results of the variation of X_{nd} with respect to the crankshaft speed for two cases: (1) I_{mv} is assumed to be a constant (1.34 A), and (2) I_{mv} varies according to the experimentally measured values (Table 2). In case (1), the angle X_{nd} increases rapidly and reaches a large value starting from the medium crankshaft speed region (approximately 1500–2000 rpm). This would lead to a sharp decline in the delivery flow rate of the HPP even before the engine reaches the high load and speed region, and this trend is inconsistent with the actual operation of the CR injection system. In case (2), a substantial change in X_{nd} appears at higher crankshaft speeds (n_{eng} > 2000 rpm). Thus, the assumption of I_{mv} = const can lead to significant deviations regarding the filling state of the HPP, thereby reducing the accuracy of the rail pressure dynamic model.

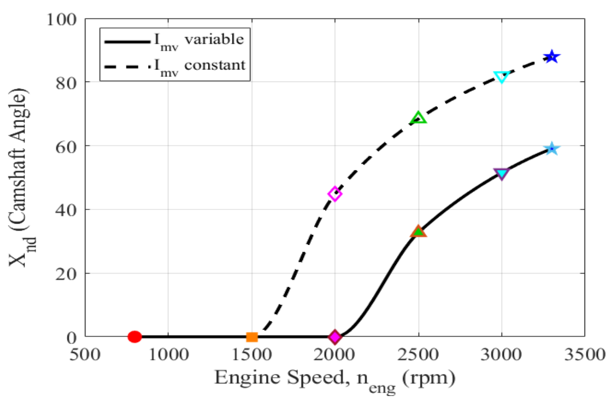

Figure 5. *Variation of X_{nd} assuming I_{mv} is a constant and under ECU regulation*

When calculating for case (2), in the low-speed region (n_{eng} < 2000 rpm), as the piston moves downward, the filling time is sufficient for the fuel to completely fill the cylinder chamber volume before the piston begins its compression stroke. Consequently, the pressure inside the cylinder increases rapidly and reaches the required pcr value almost immediately at the start of compression (Xnd = 0°). Under this condition, the actual delivery flow rate of the HPP is close to the theoretical flow rate value. As the speed increases to 2500 rpm (the engine speed region where maximum torque is achieved), the filling time gradually decreases, and the fuel cannot completely fill the cylinder chamber. As a result, a "non-useful" compression interval appears before the pressure reaches the pcr level (Xnd ≠ 0°). In the speed range of 2500–3300 rpm, Xnd increases almost linearly with the engine speed, and Xnd = 59° at neng = 3300 rpm. This aligns with the actual suction, expansion, filling, and vaporization process of diesel fuel in the HPP. At the beginning of the suction phase, the clearance volume above the piston crown contains liquid fuel at a pressure equal to the rail pressure. As the piston moves downward, the cylinder volume increases, and the remaining liquid fuel expands to accommodate the volume increase, reducing the fuel pressure inside the cylinder. At a certain piston position, the fuel pressure will drop below the supply pressure from the MV, and fuel is drawn into the cylinder. If the HPP camshaft speed exceeds a limit value, the piston will reach the BDC before the cylinder chamber volume is completely filled with fuel [19]; therefore, the cylinder chamber is only partially filled, and a fuel vapor region will appear. As the piston moves upward, this vapor must completely condense before the fuel begins to be compressed to the rail pressure, which delays the start of fuel delivery and causes Xnd to increase with engine speed.

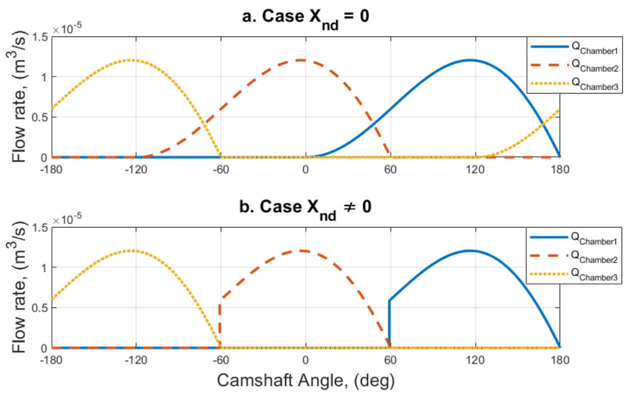

Figure 6. *Variation of the delivery flow rate of the three pump elements when X_{nd} = 0° (a) and X_{nd} = 59° (b)*

The calculated results of the variation of the delivery flow rate of the three pump elements according to the camshaft angle, corresponding to X_{nd} = 0° and X_{nd} = 59°, are presented in Figure 6. It can be observed that each pump element generates a half-sine wave flow pulse, phase-shifted by 120°, which accurately reflects the structural design of the HPP. Thanks to this phase-shifted distribution, the total flow rate delivered into the CR is more continuous, contributing to the reduction of p_{cr} oscillations and ensuring the stable fuel delivery capability of the fuel injection system. When X_{nd} = 0° (Figure 6a), the three pump elements operate fully throughout the entire compression stroke; therefore, the delivery flow rate reaches its maximum value in the middle region of the compression stroke. Meanwhile, with X_{nd} = 59° (Figure 6b), a portion of the compression stroke does not perform the fuel delivery process. These simulation results are consistent with the published research results of other authors [11], [20].

A summary of the effect of X_{nd} on the delivery flow rate of the HPP (Q_{hpp}) corresponding to three engine speed values, n_{eng} = 2000, 2500, and 3300 rpm, is presented in Figure 7. The graphs demonstrate a distinct variation in Q_{hpp} corresponding to different X_{nd} values. Specifically, at n_{eng}= 2000 rpm, when the system has sufficient filling time, X_{nd} = 0°, and the flow rate characteristics are almost identical to the geometric displacement law of the piston. The entire compression stroke participates in pressure generation and fuel delivery, with no interruption interval appearing during the cycle. As the speed increases to 2500 rpm, the deficit in filled fuel causes the flow wave to begin exhibiting a flow loss region at the beginning of the compression stroke, creating a double-peak waveform during a single delivery event. This flow reduction region continues to expand at n_{eng} = 3300 rpm; at this point, the delivery pulse width is significantly narrowed, causing sharp flow drop intervals between cycles and consequently leading to a severe decline in the actual Q_{hpp} of the HPP.

This phenomenon demonstrates that the delivery characteristics of the HPP in the high-speed region are strongly dominated by the increase in X_{nd}, rendering the relationship between the flow rate and camshaft speed no longer linear. The inevitable consequence is a reduction in the average delivery flow rate of the HPP, leading to a tendency for the actual pressure in the CR to drop compared to the target setpoint value of the ECU. To compensate, the ECU is forced to adjust the p_{cr} control strategy by intervening in the operating states of the MV and PCV valves. In addition, the distortion caused by X_{nd} alters both the frequency and amplitude of the output pressure oscillations from the HPP compared to the theoretical process, causing deviations in the mean pressure value, increasing the pressure rise delay, and completely transforming the oscillation characteristics of the p_{cr} signal.

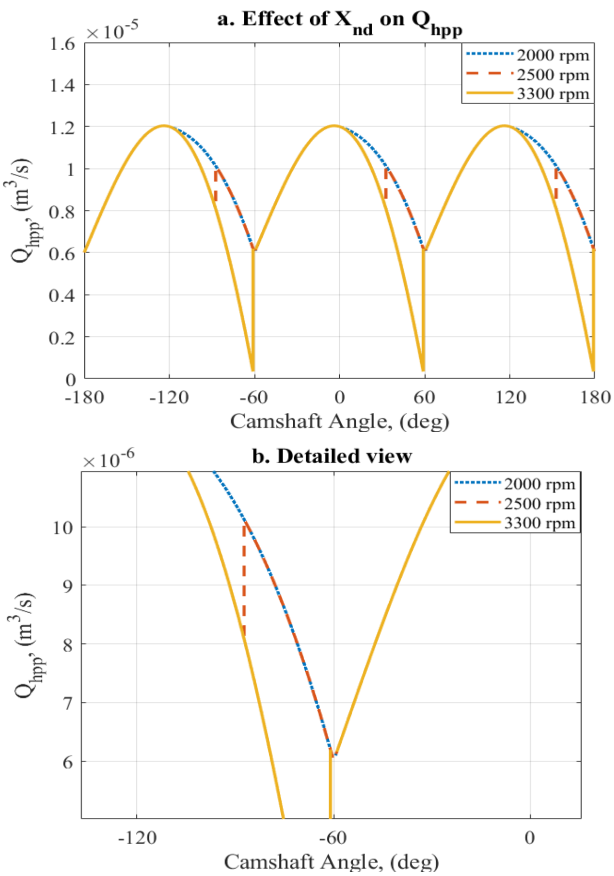

Figure 7. *Effect of X_{nd} on Q_{hpp} (a) and a detailed view (b)*

In previous studies [11], [20], diagnostic methods have often originated from the assumption that the p_{cr} signal is not completely stable but contains periodic oscillations. These oscillations arise from the discontinuous operation of the HPP and injectors, carrying characteristic frequency information (for example, the compression cycle of the HPP generates an oscillation with a period of approximately 180° crankshaft angle). Based on this, the application of Fast Fourier Transform (FFT) analysis allows the p_{cr} signal to be separated into distinct frequency components, utilizing the amplitudes to evaluate and diagnose faults in individual components. However, when considering the influence of the angle X_{nd}, the assumption of simple periodic oscillations is no longer entirely appropriate. The variation of X_{nd} severely distorts the fuel delivery process, generating discontinuous delivery phases and creating multiple sharp peaks and higher-order harmonics in the flow rate and pressure signals (Figure 7).

From the above analyses, it is evident that detailed dynamic modeling of the HPP delivery process, taking into account the X_{nd} parameter and the actual variation of the I_{mv} current according to the ECU control strategy, is essential. This approach facilitates the development of a p_{cr} dynamic simulation model with higher accuracy, establishing a solid foundation for the application of real-time MBD methods for CR diesel fuel injection systems based on the p_{cr} signal.

5. Conclusions and future work

From the theoretical and simulation research results of the CP1-H HPP characteristics on the D4CB 2.5 TCI-A engine, considering ECU intervention, the authors draw the following conclusions:

First, practical operation demonstrates that the ECU continuously adjusts the MV and PCV to optimize the intake flow rate. The control current I_{mv} fluctuates strongly and decreases sharply in the region near the rated power; therefore, the assumption of "I_{mv} is a constant" in many previous models does not accurately reflect the control nature of the system, especially in the high-speed range.

Second, utilizing the concept of the non-delivery angle X_{nd} - the compression angle interval during which the pressure in the pump element cylinder chamber has not yet overcome the rail pressure - allows for an accurate description of the incomplete fuel filling phenomenon. The variation of X_{nd} under the influence of I_{mv} is a comprehensive parameter that more faithfully reflects the actual filling state of the HPP than merely considering the valve opening parameter.

Third, the appearance and increase of the angle X_{nd} in the high-speed region severely distort the delivery flow rate characteristics of the HPP. The delivery pulse no longer maintains its theoretical sinusoidal shape but is narrowed, exhibiting multiple sharp peaks and interruption intervals, which subsequently leads to changes in the amplitude and frequency of the flow rate oscillations. This directly causes nonlinear deviations in the rail pressure signal p_{cr}.

Fourth, if the influence of X_{nd} is neglected, fault diagnostic methods based on periodic oscillation spectrum analysis of the p_{cr} signal will encounter significant errors. The integration of the X_{nd} parameter into the mathematical model is a mandatory requirement for developing a high-accuracy reference model for rail pressure dynamics.

Based on the HPP model that has successfully described the dependence of the delivery flow rate on the non-delivery angle (X_{nd}) and the control current (I_{mv}), the subsequent development directions of this research include:

Completing the closed-loop MBD diagnostic model: The HPP model established in this work will be integrated with dynamic sub-models of the CR, pressure control valve (PCV), and fuel injectors to form a comprehensive "closed-loop" reference model for the entire high-pressure circuit. Crucially, all components will be synchronized within the crank angle domain to calculate instantaneous rail pressure fluctuations (p_{cr}). This integrated framework will serve as the engine for a real-time MBD algorithm by evaluating the residuals generated between the predicted and actual p_{cr} signals.

Experimental validation using high-speed DAQ: To overcome the low-frequency sampling limitations of standard OBD-II (ELM327) interfaces, future experiments will utilize high-speed data acquisition systems (DAQ) capable of capturing pressure waveforms at frequencies above 2 kHz. This will allow for the validation and calibration of the overall model against actual high-frequency pressure ripples, ensuring that the predicted effects of X_{nd} are accurately reflected in the diagnostic system.

Experimental fault diagnosis on test bench: Diagnostic experiments will be conducted by inducing artificial faults on the engine test bench - such as high-pressure circuit leakages, a stuck PCV, or clogged injectors. These tests aim to evaluate the sensitivity, reliability, and fault isolation capability of the proposed diagnostic system under controlled, real-world conditions.

Expanding the scope of investigation: Subsequent studies will investigate the behavior of X_{nd} under transient engine conditions to move beyond steady-state analysis. Additionally, the research will explore the variation of X_{nd} and HPP characteristics when utilizing alternative fuels with different physical properties, such as biodiesel, which can significantly alter the volumetric efficiency and filling dynamics of the pump.

REFERENCES

[1] K. Reif, *Diesel Engine Management: Systems and Components*. Wiesbaden, Germany: Springer Vieweg, 2014.

[2] K. V. Nguyen, T. A. Trung, and N. H. Vu, "Experimental study of the effects of biodiesel on characteristics pressure of a commonrail diesel fuel injection system", *Journal of Science and Technology in Civil Engineering*, vol. 11, no. 4, pp. 52-57, 2017.

[3] N. H. Vu, T. T. Tuan, and P. T. Kien, "Determination of the fuel injection pressure change of the CommonRail diesel fuel injection system on a chassis dynamometer", *Vietnam Mechanical Engineering Journal*, no. 302, pp. 143-139, 2023.

[4] S. Simani, C. Fantuzzi, and R. J. Patton, *Model-based Fault Diagnosis in Dynamic Systems Using Identification Techniques*. London, UK: Springer-Verlag, 2003.

[5] S. X. Ding, *Model-Based Fault Diagnosis Techniques: Design Schemes, Algorithms and Tools*, 2nd edition. Duisburg, Germany: Springer, 2013.

[6] R. Isermann, "Advanced model-based diagnosis of internal combustion engines", in *Internationaler Motorenkongress*, Germany, 2016, pp. 413-432.

[7] K. V. Nguyen, L. A. Vu, T. V. Thoan, T. A. Trung, and N. H. Vu, *Research on controlling common rail diesel engines using biodiesel*, Vietnam: Natural Science and Technology Publishing House, 2020.

[8] S. Clever and R. Isermann, "Model-based fault detection and diagnosis for common-rail injection systems", *MTZ worldwide*, vol. 71, no. 2, pp. 32-39, 2010. https://link.springer.com/article/10.1007/BF03227006.

[9] L. D. Thi, P. X. Phuong, N. H. Vu, N. X. Dat, N. H. Hiep, L. T. Duong, "A study on common rail injector diagnosis of diesel engine", *Vietnam Mechanical Engineering Journal*, no. 3, pp. 152-156, 2020.

[10] T. T. Tuyen, N. X. Dat, N. H. Vu, "Studying pressure fluctuation in a common rail fuel injection system operating under solo injection strategy", *Vietnam Mechanical Engineering Journal*, no. 1+2, pp. 55-65, 2022.

[11] P. Sauer, *"Model-Based Fault Detection and Diagnosis For The Fuel System Of A Six-Cylinder Heavy Duty Diesel Engine"*, Ph.D. dissertation, Dept. Veh. Eng., TU Darmstadt, Germany, 2021.

[12] R. Isermann, *Combustion Engine Diagnosis – Model-based Condition Monitoring of Gasoline and Diesel Engines and their Components*. Germany: Springer, 2017.

[13] A. Mulemane, J. S. Han, P. H. Lu, S. J. Yoon, and M. C. Lai, "Modeling dynamic behavior of diesel fuel injection systems", *SAE Technical Paper*, no. 2004-01-0536, 2004.

[14] R. O, et al., "Dynamic Analysis of Common Rail Injection System for Diesel Engine based on AMESim/Simulink Co-Simulation", *International Journal of Scientific Research in Science and Technology*, vol. 10, no. 3, pp. 89-107, 2023. https://doi.org/10.32628/IJSRST52310315.

[15] D. X. Nguyen, V. H. Nguyen, and P. X. Pham, "Developing and validating a GT-Suite based model for a second generation CommonRail Solenoid Injector", *Vietnam Journal of Science and Technology*, vol. 59, no. 3, pp. 390-401, 2021. https://doi.org/10.15625/2525-2518/59/3/15803.

[16] V. H. Nguyen, A. Cavicchi, D. X. Nguyen, N. T. Kien, P. X. Phuong, L. Postrioti, "Hydraulic characterization of a second-generation common rail injector operating under solo and split injection strategies", *Flow Measurement and Instrumentation*, vol. 85, pp. 102-170, 2022. https://doi.org/10.1016/j.flowmeasinst.2022.102170

[17] P. Q. Thai and H. D. Tri, "Application of fuzzy logic for fault diagnosis of the engine fuel system of hamm roller". *The University of Danang - Journal of Science and Technology*, vol.18, no.5.1, 2020. ISSN: 1859-1531.

[18] R. Bosch, *Software Documentation Basis Y445 S00 148*, November 2000.

[19] K. V. Nguyen, T. A. Trung, and N. H. Vu, "Modeling a Commonrail Diesel Fuel Injection System", *Vietnam Mechanical Engineering Journal*, September, pp. 39-44, 2016.

[20] R. Isermann, *Engine Modeling and Control: Modeling and Electronic Management of Internal Combustion Engines,* Germany: Springer, 2014.

[21] W. Niklawy, M. Shahin, M. Amin, and A. Elmaihy, "Modelling and experimental investigation of high-pressure common rail diesel injection system", *IOP Conference Series: Materials Science and Engineering*, vol. 973, no. 1, p. 012037, 2020.

[22] K. V. Nguyen, "*Research on controlling CommonRail type diesel fuel injection system when using diesel-biodiesel fuel mixture*", Ph.D. dissertation, Hanoi University of Science and Technology, Hanoi, Vietnam, 2019.

[23] K. Prinz, W. Kemmetmüller, and A. Kugi, "Mathematical modelling of a diesel common-rail system", *Mathematical and Computer Modelling of Dynamical Systems*, vol. 21, no. 4, pp. 311-335, 2015.